Journal of Applied Polymer Science

Effects of antimicrobial agents on the thermal and mechanical properties of acrylate hydrogel matrices

Pierrick Paillot,[1,2,3] Corinne Jegat,[1,2,3] Frédéric Becquart,[1,2,3] Mohamed Taha[1,2,3]

[1]Université de Lyon, F-42023 Saint-Etienne, France
[2]CNRS, UMR 5223, Ingénierie des Matériaux Polymères, F-42023 Saint-Etienne, France
[3]Université de Saint-Etienne, Jean Monnet, F-42023 Saint-Etienne, France
Correspondence to: J. Corinne (E-mail: corinne.jegat@univ-st-etienne.fr)

ABSTRACT: Polymer materials with antimicrobial activity are prepared by UV polymerization of acrylate and methacrylate mixture at room temperature. The antimicrobials are silver acetate and copper (II) acetate, used without pretreatment. Their chemical stability in the acrylate matrix and their effect on the thermal and mechanical properties of the polymer matrix are investigated as a function of their concentration up to 15 wt %. Physico-chemical, thermal, rheological, and morphological analyses as well as the surveillance of metal salts release in aqueous medium are conducted. A significant decrease in the thermal stability of the salts introduced into the acrylate matrix is observed after UV treatment. The metal salts also have significant effects on the properties of the matrix. A plasticization and densification of the material associated with an aggregation of salts up to the percolation at the highest concentration are highlighted. At equal concentrations, the effects are more pronounced in the presence of copper salts. The latter was released more slowly than silver salts from acrylate material. © 2016 Wiley Periodicals, Inc. J. Appl. Polym. Sci. **2016**, *133*, 43501.

KEYWORDS: coatings; composites; mechanical properties; photopolymerization; thermal properties

Received 9 October 2015; accepted 1 February 2016
DOI: 10.1002/app.43501

INTRODUCTION

Acrylate hydrogels are materials with many advantages, which explain their particularly frequent use in medical and biomedical domains, or more specifically for contact lenses. They are biocompatible with a low toxicity, so they represent a safe material for any user or consumer. Another important advantage is their high swelling capacity in particular environments, for example, with aqueous solutions with high humidity levels.[1–4]

Hydrogels may be synthesized according to different polymerization methods (gamma ray, UV light, and heat application) to finally obtain the formation of networks. For this reason, these materials can be easily integrated in an industrial process.[5,6]

The antimicrobial activity of hydrogel materials can be obtained relatively easily by dispersing the agent in acrylate monomer solutions[7–9] or after polymerization, by immersing the hydrogel in an aqueous solution with an active agent.[10–12] Another possibility is to conduct a reaction between monomers and an active agent to synthesize active copolymers.[13–15] Two types of antimicrobial materials may be obtained. The first type is a material where the antimicrobial agent diffuses to be directly in contact with the bacteria and act against their proliferation. The second possibility is to elaborate a material with active sites grafted in the polymer matrix. In this case, the pathogen germs will come in contact with the active sites, which will have a bactericidal action.[16–19]

Different antimicrobial agents have been used in the past such as antiseptics (fluorescein, ciprofloxacin, Chlorhexidine, diacetate, Gatifloxacin, ...),[20–23] oxides (zinc oxide),[24,25] peptides (maximin lipopeptide-4),[9,26] antimicrobial polymers (chitosan, polyvinylpyrrolidone, ...),[27] or metal compounds (nanometric particles or silver nitrate).[28–31]

In our previous study, antimicrobial activity of acrylate hydrogels with copper acetate and silver acetate as agent, introduced before polymerization, has been demonstrated and compared with 17 other molecules.[32] These metallic salts obtained one of the best activities. Several families of pathogens have been tested: *Pseudomonas aeruginosa*, *Staphylococcus aureus*, or *Aspergillus brasiliensis*. These different microbial compounds represent germs susceptible to proliferate in cosmetics products.

The antimicrobial activity of metal particles, such as silver or copper, is known but their action mechanism is not yet fully understood. Very probably, the metal acts as an active agent under its ionic form (Ag^+ for silver, for example) in a moist environment.[33,34] These ionic compounds will come into

contact with the cell walls of microbes and will act on their integrity to prevent proliferation. Presently, metallic salts are mainly used as sources of ions to generate elementary nanometric particles before their dispersion in materials and to obtain antiseptic effectiveness. The direct dispersion of salts in materials prevent any contact between metallic nanoparticles and the human body and could be a safe alternative for antimicrobial materials elaboration. Moreover, a partial redox reaction between cationic silver or cationic copper and anionic acetate groups may occur allowing the formation in situ of a neutral solid filler.

The objective of this work is to evaluate the impact of copper (II) acetate and silver acetate on acrylate matrices properties obtained by UV polymerization. In particular, the effects on the thermal properties, visco-mechanical characteristics, morphological aspects, and release behavior of the two salts and their respective concentrations will be studied. To the best of our knowledge, very few studies have focused on the effect of antimicrobial agents on these polymer matrix properties. Our materials will be used to protect strategic areas of cosmetic packaging with the treatment of a thin film coating.

MATERIALS AND METHODS

Materials

2-hydroxyethyl methacrylate (HEMA, purity 97%), silver (purity > 99%), and copper (II) acetates (purity 98%) and polyethylene glycol dimethacrylate (PEGDMA $n(O{-}CH_2{-}CH_2) = 550$), benzophenone (BP), and 2,2-diethoxyacetophenone (DEAP) were purchased from Aldrich and used as received without further purification. The tertiary amine was an experimental product (CN381) and kindly delivered by Sartomer.

Synthesis of Acrylate Films

The photo initiating system was a homogeneous solution composed of 60 wt % tertiary amine (CN381), 20 wt % benzophenone (BP), and 20 wt % 2,2-diethoxyacetophenone (DEAP). The two monomers—poly (ethylene glycol) dimethacrylate (PEGDMA) and 2-hydroxyethyl methacrylate (HEMA)—were mixed with a mass ratio of 70:30, respectively. To this blend, an equivalent of 5 wt % of the photoinitiating system was added. The antimicrobial agent was dispersed in the monomer mixture with different mass concentrations equal to 5, 10, and 15 wt % prior to the photoinitiating system addition (% relative to total blend). All blends were prepared in a glass beaker under magnetic stirring.

The irradiation system was a U.V. light (Banc Fusion UV system F300S (fusion system)) associated with a conveyor belt to pass the sample under the U.V. lamp with wavelengths between 220 and 300 nm. The wavelengths and dose measurements were assessed by a system named Power puck UV radiation (UV Power puck II from EIT Company). The prepared blends were spread on an poly(ethylene-co-vinyl alcohol) support with a bar coater and placed on the conveyer belt. The irradiation step was carried out at room temperature and repeated 5 times for an optimal curing of the monomer solution and finally to obtain the network. Thus, the resulting system is a polyacrylate coat with a thickness of around 100 μm. The adhesion between the support and the polymethacrylate matrices was low, so easily separable.

Characterizations

Thermal Analysis by DSC. Differential scanning calorimetry (DSC) measurements were carried out with a Q10 calorimeter from TA Instruments. The samples with masses between 3 and 4 mg were transferred to hermetic pans, sealed, and analyzed from −80 to 200 °C with a heating rate of 10 °C min^{-1} (2 cycles). Cycle 1 = −80 to 200 °C with a heating rate of 10 °C min^{-1}, then cooled to −80 °C at 10 °C min^{-1}, and then heated to 200 °C with a heating rate of 10 °C min^{-1} (Cycle 2). The glass transition temperatures were collected as the inflection points.

Thermogravimetric Analysis by TGA. A thermogravimetric analyzer (TGA) from Mettler Toledo, TGA/DSC 1, was used. Thermal degradation experiments were done under nitrogen purge with a flow rate of 80 mL·min^{-1} for all experiments. Samples ranging from 15 to 20 mg were heated from 30 to 500 °C with a heating rate of 10 °C·min^{-1}.

DMTA Measurements. The dynamic mechanical thermal analyses of the PEGDMA/HEMA network films were performed with Rheometrics Solids Analyzer (RSA II, TA-Instruments) to obtain tensile dynamic mechanical spectra. The samples were cut with a predetermined shape (40 × 10 × 100 μm) from the synthesized samples. For dynamic tensile measurements, a nominal strain at 0.1% was fixed, with an applied frequency of 1 Hz. Storage modulus E', loss modulus E'', and loss factor tan δ were determined as a function of temperature. Data were taken from −50 to 100 °C using a heating rate of 3 °C·min^{-1}. Each sample was equilibrated in the same chamber under dry nitrogen at the starting temperature prior to running the test.

Observation of Morphologies by Scanning Electronic Microscopy. SEM (HIROX SH 4000M Scanning electron microscope) was used to observe the morphology of the different surfaces of the films. The surface of each sample was covered with a gold–palladium layer prior to analysis (DENTON VACUUM DESK V: 40 mA/30 s).). The size of the dispersed phase was evaluated with "Image J" software.

Release of Antimicrobial Agents. The release kinetics of the antimicrobial agents from an immerged piece of PEGDMA: HEMA (wt % ratio fixed at 70:30) matrix in 10 ± 0.02 g of reference water (Distilled Water used for standard curves) was followed for several hours by UV spectroscopy (Agilent Technologies Cary Series 100 UV–VIS Spectrophotometer) at room temperature and under magnetic stirring. The volume of each sample was equaled to approximately 18.2 ± 4.8 mm^3 and with masses between 19 and 32 mg.

The methacrylate matrices presented very small quantities of residual monomers and photoinitiator but according to our calibration curves carried out in the same conditions, they absorbed 5–10 times more than the antimicrobial agents. So it was necessary to correct the measured absorbance at 224 nm. The UV absorbance at 224 nm generated by the residual photoinitiator and monomers has been determined on the release solutions from samples of PEGDMA:HEMA (wt % 70:30) matrix

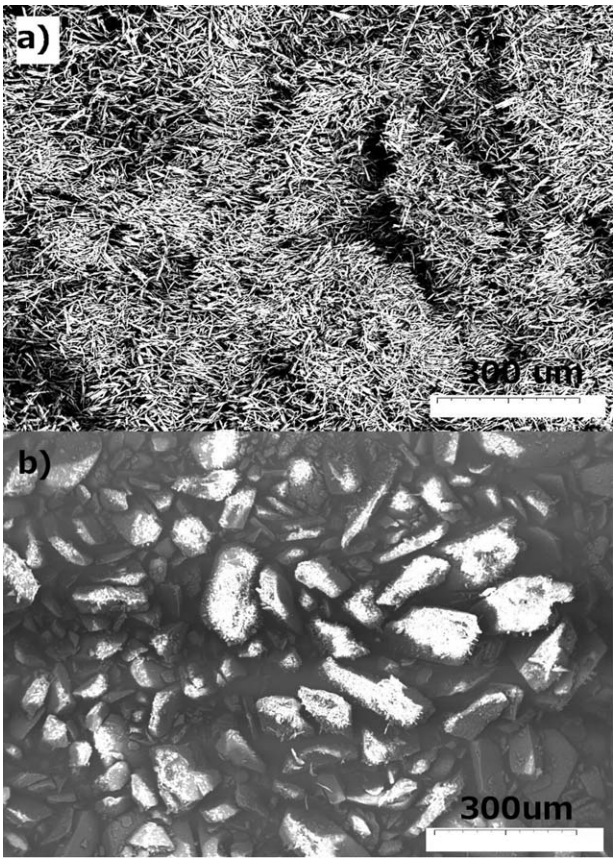

Figure 1. SEM images (**100×**) of (a) silver acetate powder and copper (II) acetate powder.

but without metallic salt (blank test). This correction allowed the evaluation of metallic salts release by minimizing masking effects of the photoinitiator and the monomer. All the standard solutions were prepared by dissolving silver acetate and copper (II) acetate in water with accurately known concentrations. So the absorbance measurement reflected the antibacterial salt agents' concentration.

Density Measurements. The determination of densities of the methacrylate matrices was done by measuring the dimensions of each sample associated with a measure of weight. Dimensions were measured with an Otelo® digital caliper 0–150 mm. The thicknesses were measured with an elcometer. Weight was obtained with a precision of 0.1 mg.

RESULTS AND DISCUSSION

The metallic salts used as antimicrobial agents in this work are powders. Characteristics of these powders have been analyzed and reported before the study on the impact of the salts dispersion on the physicochemical, thermal, rheological, and releasing properties of an acrylate matrix elaborated from blend PEGDMA/HEMA (70/30).

Characteristics of the Antimicrobial Agents

The silver acetate powder was mostly needle-shaped with a shape factor of about 12 (average length = 30 μm and average width = 2.5μm). The copper (II) acetate powder had a shape factor closer to 1 with a size of around 5.1 μm but highly agglomerated in large grains with an approximate dimension of 76 μm (Figure 1). The densities of these powders were respectively equal to 3.26 g cm^{-3} and 1.88 g cm^{-3} for silver and copper. These values were higher than the density of the neat acrylate matrix (1.29 g cm^{-3}).

The thermal stability of the metallic salts was verified by TGA analysis. The results are summarized in Table I.

The loss of weight of two salts was initiated around 180 °C and was terminated at 290–300 °C but it was not total. For the silver acetate, only one step of thermal degradation was observed with a weight loss equal to 35%. By contrast, 3 steps of decomposition around 270–300 °C were observed for copper acetate and for each step, the compound lost approximately 23 wt %. The total decomposition of acetate groups can be considered and verified from the calculation of the relative mass proportion of acetate group in the salts, which is equal to 35% in silver salt and 65% in copper salt. The weight losses determined from TGA analysis correspond fairly well to the initial relative proportion of acetate in the salts.

These results are in agreement with those in the literature.[36,38–40] According to Logvinenko *et al.*,[36] an intramolecular reduction of silver ions in smaller metallic particles ($Ag^{+}\rightarrow Ag0$) occurs with a release of CO, H_20, CO_2, CH_3COOH, and small quantities of radicals during the decomposition process. Beyond 300 °C, a recrystallization of fine metallic particles with a porous structure and the formation of oxides were recently characterized by XRD, FE-SEM, TEM, and XPS techniques.[37] The particles' size of the Ag nanocrystals was in the range of 10–35 nm. The decomposition of copper salts is more complex ($Cu^{2+}\rightarrow Cu^{+}\rightarrow Cu0$) and poorly studied.[39,40]

Table I. Thermal Stability of Silver Acetate and Copper (II) Acetate (Pure Compounds)

Powder	Degradation steps number [30–500 °C]	Degradation temperature (°C) (inflexion point)	Weight loss Δm (%)
Silver acetate	1	293	35
Copper (II) acetate	3	273	25
		288	23
		301	21
			69

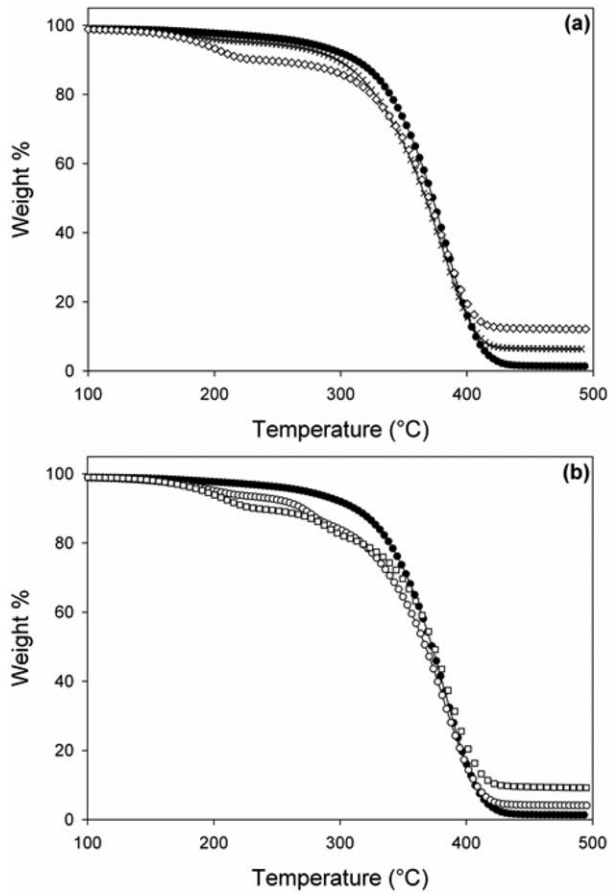

Figure 2. (a) TGA curves of PEGDMA/HEMA/(70/30) without antimicrobial agent (black dots): with 5 wt % of silver acetate (cross dots) and 15 wt % of silver acetate (white diamond dots). (b) TGA curves of PEGDMA/HEMA/(70/30) without antimicrobial agent (black dots): with 5 wt % of copper (II) acetate (white dots) and 15 wt % of copper (II) acetate (white square dots).

Effect of the Metallic Salts on the Thermal Stability of Acrylate Hydrogels

The thermal stability of acrylate films with different concentrations of metallic salts was also verified by TGA analysis. Figure 2 depicts the weight losses of samples under thermal treatment with or without 5% and 15% of metallic salts between 100 and 500 °C.

Figure 2 shows that an introduction of metallic salts in an acrylate matrix prevents the total degradation of materials with the presence of residual components at the highest temperatures while the neat matrix undergoes a complete degradation. Two to three steps of degradation were observed which can be attributed to the filler for the first steps and to the acrylate matrix for the last step. A range of about 100–110 °C was noted between the first steps and the last. For the matrices with 5 and 15 wt % of silver acetate, the weight losses at the first step corresponded to the quasi amount of salts introduced in the matrix. Similar results were found for the matrix with 5 wt % and 15% of copper (II) acetate. Figure 3 highlights the impact of the matrix on the salts' thermal stability and conversely, the impact of the salts' presence on the thermal stability of the acrylate film. A weakening of the salts' thermal stability in the matrix was observed. The neat salts are decomposed around 270–290 °C, while in acrylate films, the decomposition temperature is decreased in the 210–220 °C range. On the other hand, the decomposition temperatures of the polymer matrix, which correspond to the last step, are not significantly modified by the presence of metallic salts. So, metallic salts did not seem to interfere with the polymerization and cross-linking between the two monomers. An intermolecular interaction between the metallic salt and the acrylate matrix such as the coupling force and hydrogen bonding between the Cu ($CuSO_4$) and the hydroxyl groups of HEMA observed by Liu *et al.*[41] is not probable in our acrylate films.

It was identified that the salt degradation at 200 °C was clearly at lower temperature than the pure salts (300 °C). This is attributed to the matrix effect. Ionic interactions between acetate and silver ions were lowered when they were dispersed in methacrylate matrix. In addition, metallic salts degrade under UV irradiation applied during the process of fabrication leading to degradation at lower temperature. These effects were also mentioned in literature.[42,43]

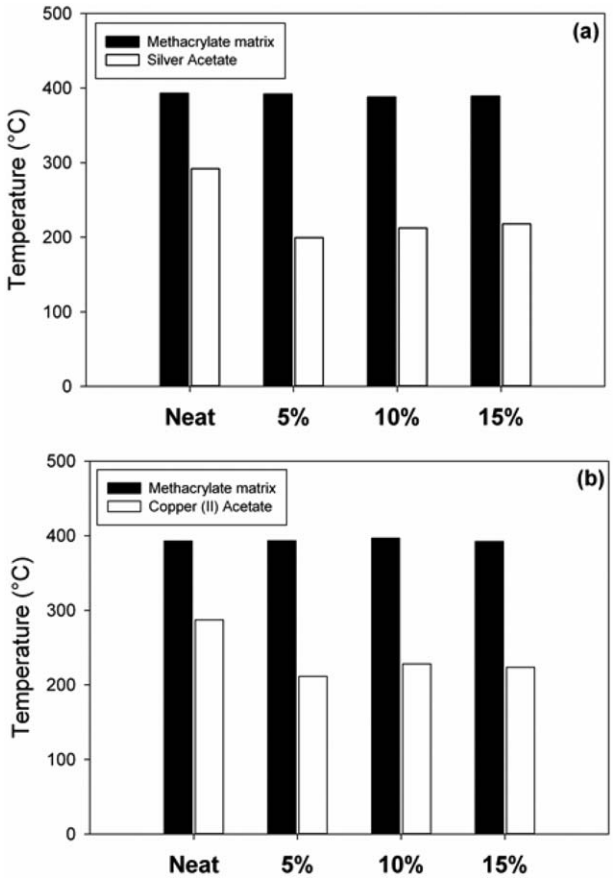

Figure 3. Decomposition temperatures of the metallic salts and the methacrylate matrices under their neat form and in blend with 5, 10, and 15 wt % of metallic salts: (a) silver acetate; **(a)** copper (II) acetate. The decomposition temperature is the degradation temperature of materials determined as the midpoint of TGA curves. It corresponds to the temperature at which the mass reduction represents 50% of the global weight of component analyzed.

Table II. Glass Transition Temperature of PEGDMA/HEMA (70/30) Matrix with Different Mass Concentrations of Silver Acetate

Silver salt concentration (wt %)	T_g heating cycle 1 (°C)	T_g heating cycle 2 (°C)	Delta T_g heating cycles 1 and 2 (°C)
0	−7.2	−14.8	−7.3
5	−14.3	−24.1	−9.8
10	−11.9	−27.7	−15.7
15	−10.8	−31.5	−20.7

Effect of the Metallic Salts on Thermal Properties

The thermal properties of the matrix with different concentrations of metallic salts, determined by DSC analysis, are summarized in Tables II and III. The samples were analyzed from −80 to 200 °C with a heating rate of 10 °C min^{-1}. Two cycles of heating were done and the T_g temperatures were obtained from the inflection points. The first heating cycle was carried out to evaluate the impact of the metallic salts on the T_g of polymethacrylate matrices.

Glass transition temperatures are much lower than polymerization temperatures under UV irradiation. Without salts, the glass temperature of PEGDMA/HEMA (70/30) matrix is observed at −7 °C for the first heating cycle and −14 °C for the second heating cycle. The difference was attributed to the small degradation of the organic matrix, observed by TGA with a weight loss of 2% at 200 °C. In the presence of metallic salts, these glass transition temperatures decrease further. This effect is more pronounced after a first heating cycle and depends on salt concentrations. For the copper salt, the correlation between glass transition temperature T_g and concentration was clearly observed for each cycle. For the highest salt concentration, the T_g lowering reaches −29 °C. The difference of T_g observed between the two cycles is probably caused by a partial reduction of the metallic salts under thermal treatment around 200 °C, as mentioned before, with weight loss due to acetic acid evaporation. The thermal properties of analyzed material were consequently modified during the second DSC run.

It is known that the shape, size, toughness, and covalent or noncovalent surface interactions of fillers with matrix may induce T_g changes. Increase and decrease of T_g value can be obtained.[44] The change depends strongly on surface effects; the matrix T_g can decrease when the filler is soft as well as with the mobility of the polymer at the polymer–filler interface or when polymer–filler interactions are weak.[45] The T_g changes can also be related to interface and surface energies,[46,47] a reduction of cross-linking density of the polymer matrix,[48] an aggregation of filler[49] or even residual solvents.[50]

In this study, the polymerization was carried out without solvent; very small quantities of residual monomers were present but the reduction of cross-linking density is not probable because, according to TGA results, the thermal stability of the polymer matrix is conserved in the presence of salt. However, the conversion of metallic salts into metallic silver or copper generated by the first heating cycle at 200 °C in the DSC can cause changes in the filler/polymer interface, especially at the higher concentrations. As this study focuses on thin acrylate films, it can be considered that the effects are even more pronounced after a thermal solicitation of 200 °C. In addition, exchange reactions between small molecules formed during thermal reduction and acrylate matrix are probable causes.[51]

Effect of the Metallic Salts on Thermomechanical Properties

The thermomechanical properties of acrylate materials with 5 and 10 wt % of silver acetate and copper (II) acetate were determined by DMTA analysis (tensile mode). Figure 4(a,b) depicts the storage moduli measured as a function of the temperature between −40 and 100 °C for the two samples' series. The curves of storage modulus show an increasing of values E' at glassy state (<20 °C) and rubbery state (>40 °C). This change was lower at the glass state than at the rubbery state and especially in the presence of copper (II) acetate.

T_α was determined from tan δ and the values are reported as a function of temperature for the two samples' series [Figure 5(a,b)]. Their values are also presented in Tables IV and V. Figure 5(a,b) clearly reveals the lowering and the widening of tan(δ) peak when the concentrations of metal salts increase. This trend is particularly pronounced with the copper salts.

So, the T_α value (Tables IV and V) of filled matrices decreases by 5–20 °C compared to that of the initial acrylate matrix. The highest reduction was also observed with copper (II) acetate.

Table III. Glass Transition Temperature of PEGDMA/HEMA (70/30) Matrix with Different Mass Concentrations of Copper Acetate

Copper salt concentration (wt %)	T_g heating cycle 1 (°C)	T_g heating cycle 2 (°C)	Delta T_g heating cycles 1 and 2 (°C)
0	−7.2	−14.8	−7.3
5	−8.4	−21.8	−13.5
10	−12.9	−35.1	−22.2
15	−16.8	−43.8	−27.1

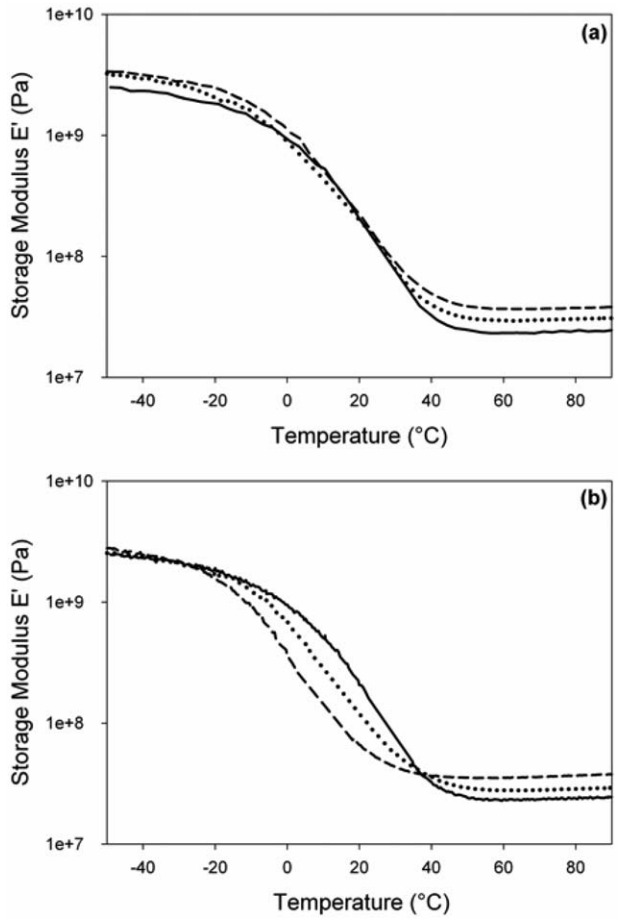

Figure 4. (a) Storage modulus E' of PEGDMA/HEMA (70/30) without antimicrobial agent (full line); with 5 wt % (dotted line) and 10 wt % of silver acetate (dash line) as a function of temperature. (b) Storage modulus E' of PEGDMA/HEMA (70/30) without antimicrobial agent (full line); with 5 wt % (dotted line) and 10 wt % of copper (II) acetate (dash line) as a function of temperature.

These DMTA results are in good agreement with DSC results even if differences between the temperature values appear according to technical analysis (DSC or DMTA). The main reason concerns the test conditions that are different; DSC was performed with a static solicitation while DMTA was dynamic. When subject to mechanical stresses, the polymer chains of network relax in different ways. The T_α taken at the tan (δ) maximum is associated to the glass transition "T_g".

In fact, the filled matrices have a higher hardness associated with an enhancement of the damping capacities. These results have demonstrated plasticizing effects (reduction of relaxation temperatures) with better mechanical properties (higher storage modulus for each state of acrylate materials). Therefore, why does the matrix loaded with metallic salts exhibit lower T_g (or T_α) and higher E' values in the rubbery and glassy regions than those of the neat methacrylate networks? Regarding the increase of the storage modulus, this effect is caused by the introduction of fillers, which generally generates the improvement of this parameter in the rubbery state. In Figure 5(a,b), a little shoulder of tan(δ) peaks toward lower temperature and what is more, a decrease of intensities and a broadening of tan(δ) peaks appear when the quantity of metallic salts increases. As for the offset of T_α, this phenomenon is more important concerning the copper (II) acetate and can be explained by a strong aggregation of salts.

The literature is poor on the subject but some works have discussed the question, in particular, Cho *et al.* in 2006[52] who studied the impact of inorganic molecules on the viscoelastic behavior of different systems (acrylate/methacrylate-based polymers or epoxy-based polymers). First, the authors have interpreted this behavior as an increase of the density of the polymer network with the formation of more flexible siloxane nodes. Suriati *et al.*[49] have observed a T_g decrease with storage modulus increase and an anomalous increase of the coefficient of thermal expansion after T_g in silver-filled epoxy-composites, which has been explained by an aggregation of silver at higher concentrations, especially for silver nanoparticles, which have higher surface energy than silver flakes. However, this phenomenon remains difficult to explain, especially in our case, because we cannot ignore the fact that the matricial polymers can react

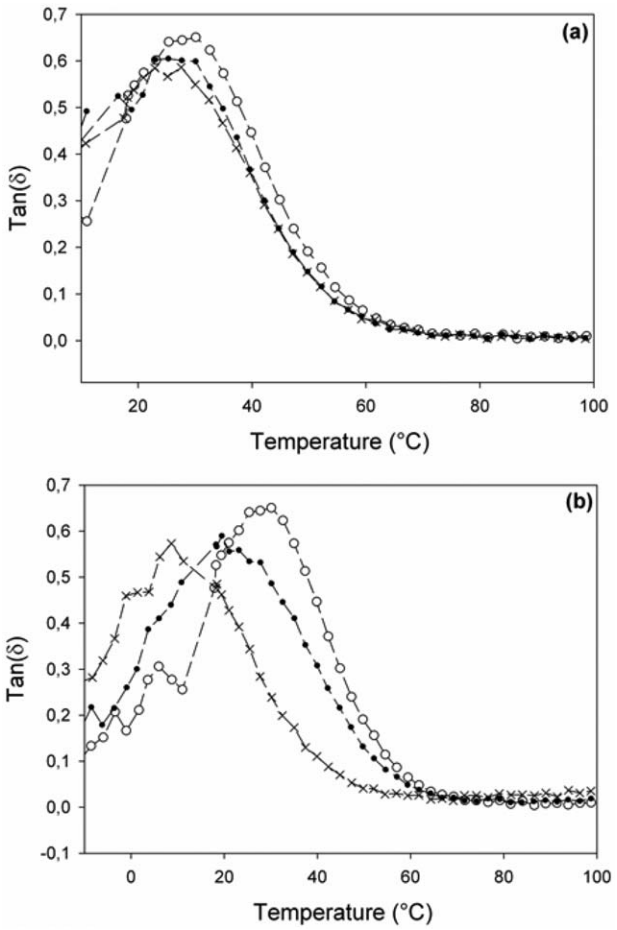

Figure 5. (a) Tan (δ) of PEGDMA/HEMA (70/30) without antimicrobial agent (white dots); with 5 wt % (black dots) and 10 wt % of silver acetate (cross dots) as a function of temperature. (b) Tan (δ) of PEGDMA/HEMA (70/30) without antimicrobial agent (white dots); with 5 wt % (black dots) and 10 wt % of copper (II) acetate (cross dots) as a function of temperature.

Table IV. T_α and Storage Modulus (in Glass and Rubbery States) of PEGDMA/HEMA (70/30) in the Presence of Silver Acetate

wt % Silver salt in PEGDMA/HEMA (70/30% wt)	T_α (°C)[a]	Storage modulus (Pa) glass state (−50 °C)	Storage modulus (Pa) rubbery state (95 °C)
0	28.7	2.49×10^9	2.50×10^7
5	24.7	3.26×10^9	3.12×10^7
10	23.8	3.39×10^9	3.82×10^7

[a] Maximum of peak of tan (δ).

Table V. T_α and Storage Modulus (in Glass and Rubbery States) of PEGDMA/HEMA (70/30) in the Presence of Copper (II) Acetate

Wt % Copper salt in PEGDMA/HEMA (70/30 % wt)	T_α (°C)[a]	Storage modulus (Pa) glassy state (−50 °C)	Storage modulus (Pa) rubbery state (95 °C)
0	28.7	2.49×10^9	2.50×10^7
5	18.2	2.62×10^9	2.97×10^7
10	7.4	2.75×10^9	3.82×10^7

[a] Maximum of tan (δ) peak

between each other, for instance, by transesterification between hydroxyl groups of HEMA of a chain with the ester group of HEMA of another chain, and that they may consequently participate to modulus increase.

Determination of Densities

The filler–polymer matrices' densities can be calculated from the theory of blends by eq. (1).[35] The acrylate films' densities were measured and then compared to these theoretical values (Tables VI and VII).

$$\rho_{\mathrm{pm}} = \frac{\rho ms * \rho np}{\rho np * mms + \rho ms * (1 - mms)} \quad (1)$$

Where ρ_{pm}, ρms, and ρnp are the densities of the polymer matrix, metallic salt, and neat polymer, respectively, and mms is the mass fraction of metallic salts.

Since the salts are denser than the acrylate matrix, experimental densities of blends are expected to be higher than that of the original matrix and to increase with the salts' concentration. In fact, they are higher overall than theoretical values. The largest differences are observed for acrylate films with copper acetate at the highest concentration. These results are in agreement with the storage moduli increase highlighted from DMTA results. In filler–polymer composites, a positive difference between the experimental densities and expected densities is often attributable to the nucleation of filler crystals in the loaded material.[35]

Effect of the Metallic Salts' Concentration on Polymer System Morphology

The morphologies of acrylate materials loaded with several concentrations of silver acetate and copper (II) acetate (5, 10, and 15 wt %) were verified by SEM analysis. Images in Figures 6 and 7 show the filled film surface for each sample.

As depicted on Figures 6 and 7, salt particles (white stain) appear dispersed or aggregated in all blends except for acrylate matrix with 5% of silver acetate. Observations revealed a formation of oriented aggregates. The reactants were mechanically spread on supports with a bar coater. This processing method probably induced the obtained orientations.

It seems that one of the phases is rich in polymer with metallic salt particles well dispersed and the other is rich in metallic salt aggregates and poor in polymer. For the blend with 5% of silver acetate, a homogenous dispersion of needle particles is obtained without significant change of form and size. The particles have a shape factor of 13.4 with similar dimensions, very close to that of initial crystals. For blends with 10% and 15% of silver acetate, the formation of needle aggregates growing in a specific direction with the concentration can be observed; at 10%, length = 177 μm and width = 39 μm and at 15 wt %, length = 300 μm and width = 57 μm.

All acrylate films with copper salt contain dispersed particles in the polymer matrix and concentrated aggregates; these

Table VI. Densities for PEGDMA/HEMA (70/30) Films with Silver Acetate

Silver salt (wt %)	Density (kg m^{-3}) (experimental)	Density (kg m^{-3}) (theoretical)
0	1291	1291
5	1294	1331
10	1443	1374

Table VII. Densities for PEGDMA/HEM A (70/30) Films with Copper (II) Acetate

Copper salt (wt %)	Density (kg m^{-3}) (experimental)	Density (kg m^{-3}) (theoretical)
0	1291	1291
5	1490	1312
10	1601	1333

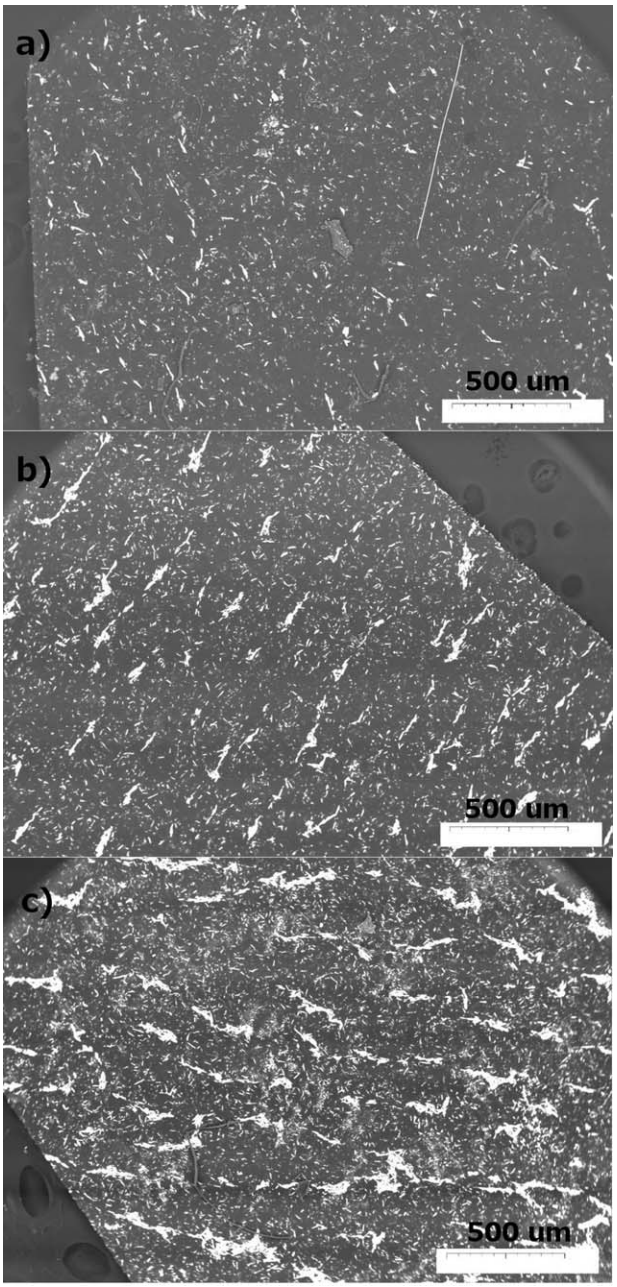

Figure 6. SEM images of polymer PEGDMA/HEMA (70/30) with silver acetate [concentration of (a) 5, (b) 10, and (c) 15 wt %] (**50×**).

aggregates grow in a preferred direction with salt concentration and seem to tend toward percolation. The shape of copper acetate particles does not seem to change in the different blends, with a shape factor of about 1 and a size of approximately 9–10 μm.

We can conclude that morphologies of the two series of acrylate blends are similar. The most highlighted difference between these series seems to be the level of percolation threshold. In the presence of copper acetate, it appears for a concentration close to 15% in the presence of copper salt while this phenomenon is much less marked at the same concentration in silver salt.

These observations are consistent with the DMTA and densities results; they confirm the aggregation effects on the T_g and the storage modulus.[52,60–63]

Release of Metallic Salts from Acrylate Blends

The objective of the test is to compare the release kinetics of metallic salts from acrylate matrix as a function of salt and of its concentration in an aqueous environment at room temperature. It has also a good interest for the final industrial application of antimicrobial packaging.

Residual photoinitiator in the polymethacrylate matrices has generated mask effects that were taken into account as before

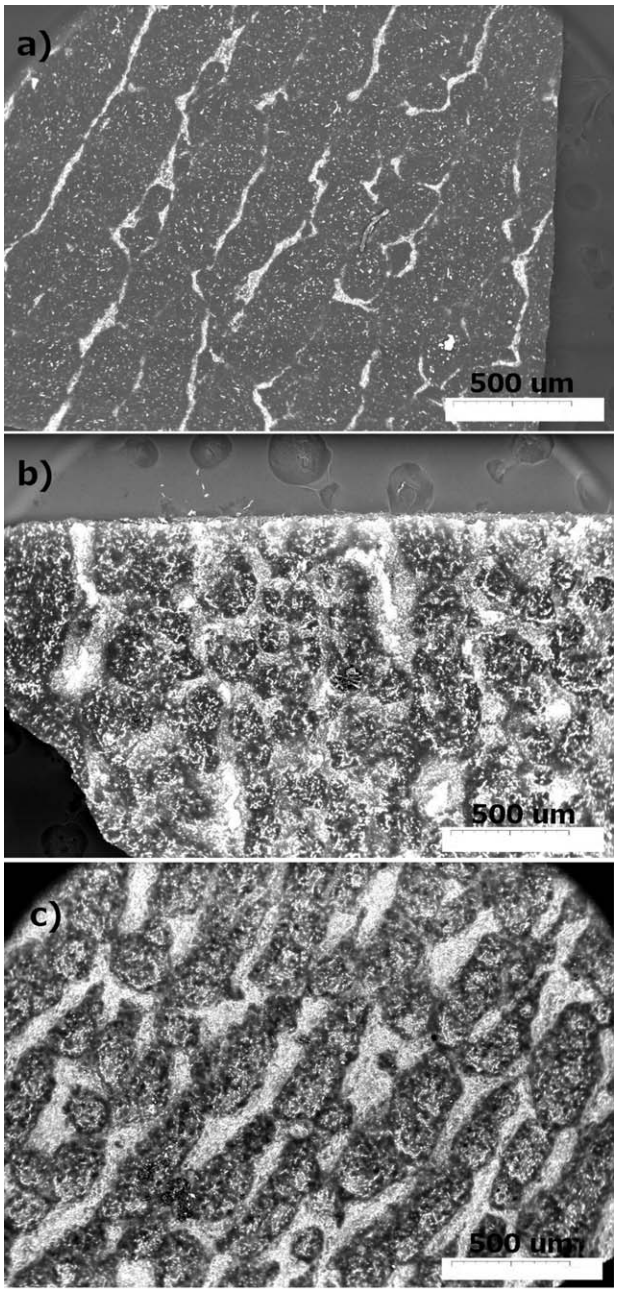

Figure 7. SEM images of polymer PEGDMA/HEMA (70/30) with copper (II) acetate [concentration of (a) 5, (b) 10, and (c) 15 wt %] (**50×**).

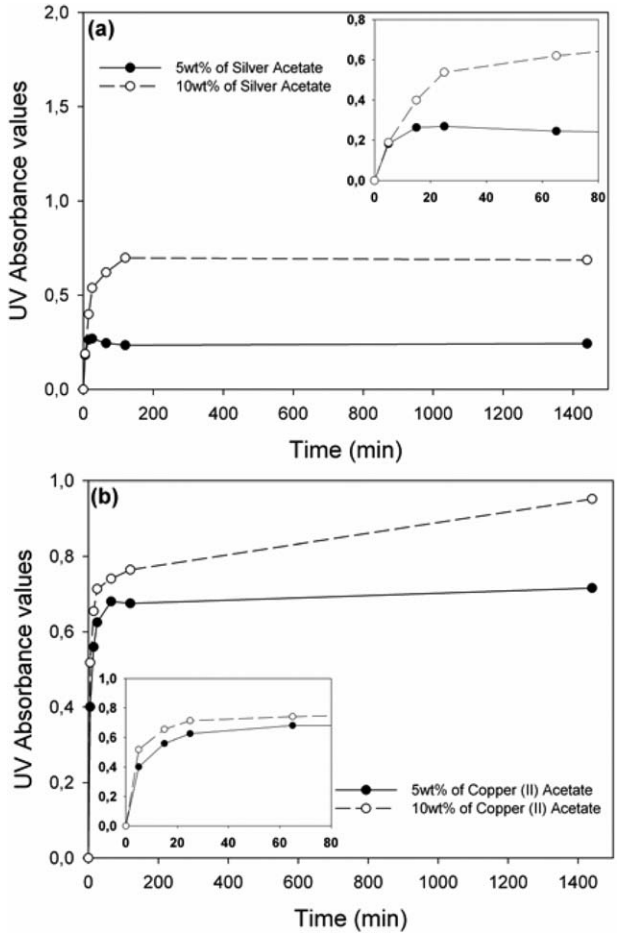

Figure 8. Absorbance values ($\lambda = 224$ nm) of released metallic salts from matrices with (a) 5 and 10 wt % of silver acetate and (b) 5 and 10 wt % of copper (II) acetate.

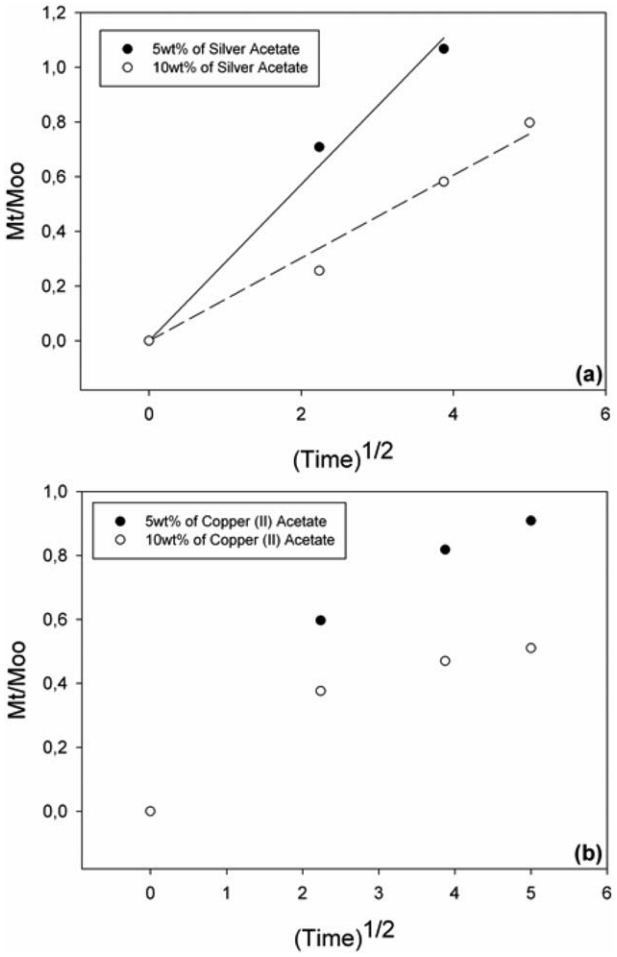

Figure 9. Verification of the Fickian law for the matrix with (a) 5 and 10 wt % of silver acetate and (b) 5 and 10 wt % of copper (II) acetate.

mentioned in the experimental part. Figure 8 depicts the UV absorbance at 224 nm after correction as a function of time for the different acrylate materials with silver acetate and with copper (II) acetate.

In the two series, the releasing of salts was very short for no evolution of absorbance was observed after an immersion in aqueous solution for 60 min. Therefore, the first conclusion is that these materials are more suitable to industrial applications with a necessity of rapid action.

Table VIII. Rate of Salts Release in Aqueous Medium at Room Temperature

PEGDMA/HEMA (70/30)	Rate of release (%)
5 wt % of silver acetate	100
10 wt % of silver acetate	100
5 wt % of copper (II) acetate	98.7
10 wt % of copper (II) acetate	67.6

Table VIII presents the rates of released agents calculated from mass ratios of released quantity upon initially introduced quantity.

For the matrices with silver acetate, the totality of antimicrobial agents was delivered after 24 h. This observation is also observed for the matrix with 5 wt % of copper (II) acetate but not with 10 wt % of copper (II) acetate. It appeared that the released rate after an immersion time of 24 h was only equal to 67.6%. In our conditions, acrylate materials release silver acetate

Table IX. Average Total Mass of Metallic Salt Released in Aqueous Medium

	Average of M_∞ (mg)	Standard deviation (mg)
5 wt % of silver acetate	0.95	0.06
10 wt % of silver acetate	2.7	0.2
5 wt % of copper (II) acetate	1.43	0.04
10 wt % of copper (II) acetate	2.9	/

Table X. Slope in the Linear Domain for Matrices with Silver Acetate

	Slope in the linear domain
5 wt % of silver acetate	0.278
10 wt % of silver acetate	0.161
5 wt % of copper (II) acetate	0.267
10 wt % of copper (II) acetate	0.155

For the matrices with copper (II) acetate, just lower concentrations are considered.

more easily than copper acetate. A verification of the Fickian law was performed and the ratio (M_t/M_∞) as a function of the square root of time is described on Figure 9. M_t represents the mass of metallic salt at a specific time t. M_∞ is the mass of metallic salts at the infinity time. Here, M_∞ was calculated by the average of each weight of salts in water measured after 60 min (except for the matrix with 10 wt % of copper (II) acetate, where M_∞ = initial mass = 2.9 mg). The results were compared in Table IX.

The results on Figure 9 show a linear relation between the ratio (M_t/M_∞) and the square root of time for a period of about 20 min for silver acetate and a much shorter period for copper (II) acetate. It can be concluded that the releasing of silver acetate from the acrylate materials follow a Fickian diffusion law in this time interval, whereas the release of copper (II) acetate deviates from the very low levels.

The slopes of the linear regression curves, given in Table X, are representative of the diffusion coefficient and can give an idea on the capacity of release. The results show that the concentrations of metallic salts also have an impact on diffusion. The diffusion coefficient decreases when concentration increases. The matrix with silver salt has a better diffusion capacity over time comparatively to copper (II) acetate for a similar concentration. These release properties are closely in agreement with the experimental densities of filled acrylate films (Tables VI and VII). Then, the density of networks is usually considered as a key factor of agent release. A denser material will have a lower diffusion capacity.[41,53–57] Finally, the deviation to Fickian behavior of copper acetate matrices could be attributed to the nucleation of filler crystals.

CONCLUSIONS

Acrylate materials with several concentrations of silver acetate and copper (II) acetate (5–15 wt %) were elaborated by UV polymerization. These salts were used because they have previously revealed an antimicrobial activity in the same materials which is interesting for industrial applications.

The main objective of this work was to evaluate the impact of these metallic salts and their concentrations on the thermal, thermomechanical, and releasing properties of acrylate thin films. Then, morphology studies were carried out to better understand the variations of these properties.

The results of this study have shown that the dispersion of silver acetate or copper (II) acetate (between 5 and 15 % w) does not modify the thermal stability but enhances the storage modulus in the glassy and rubbery states and decreases the glass temperatures T_g of the acrylate materials. Then, the thermal stability of metallic salts is weakened in acrylate matrices. The plasticizer effect could be explained by an increase of free volumes in the final matrix, which could be localized at the interface filler/polymer and could facilitate the mobility of the macromolecular chains at its vicinity. This effect increases with salt concentration. On the contrary, the enhancement of the storage modulus is linked to an increase of the density of materials with measured values higher than the densities predicted by the theory of blends. These density differences increase with salt concentration and can be attributed to the growth of filler crystal nucleates in the material. There are preferential interactions between metallic particles with intensities higher than that of polymer–salt particles interaction. Finally, this translated in a preferential network of the metallic particles and could explain the appearance of filler percolation. It appeared in this work that the density of acrylate matrix is the key factor of the releasing properties of the antimicrobial agents in an aqueous environment. The slowest release of metal salts is obtained from the acrylate matrices in which the salts were aggregated and have percolated.

ACKNOWLEDGMENTS

This work was supported through a research program titled STABIPACK II devoted to the development of antimicrobial materials for adaptation to cosmetic packaging. The research program was funded thanks to financial aids provided by FUI (Fonds Unique Interministériel) in the clusters COSMETIC VALLEY and PLASTIPOLIS.

REFERENCES

1. Toh, W. S.; Loh, X. *J. Mater. Sci. Eng. C Mater. Biol. Appl.* **2014**, *45*, 690.
2. Buwalda, S. J.; Boere, K. W. M.; Dijkstra, P. J.; Feijen, J.; Vermonden, T.; Hennink, W. E. *J. Control. Release* **2014**, *190*, 254.
3. Chirila, T.; Constable, I.; Crawford, G.; Vijayasekaran, S.; Thompson, D.; Chen, Y.; Fletcher, W.; Griffin, B. *Biomaterials* **1993**, *14*, 26.
4. Ganji, F.; Vasheghani-Farahani, S.; Vasheghani-Farahani, E. *Iran. Polym. J.* **2010**, *19*, 375.
5. Bowman, C. N.; Kloxin, C. J. *AIChE J.* **2008**, *54*, 2775.
6. Ifkovits, J. L.; Burdick, J. A. *Tissue Eng.* **2007**, *13*, 2369.
7. Tsou, T. L.; Tang, S. T.; Huang, Y. C.; Wu, J. R.; Young, J. J.; Wang, H. J. *J. Mater. Sci. Mater. Med.* **2005**, *16*, 95.
8. Krezovic, B. D.; Dimitrijevic, S. I.; Filipovic, J. M.; Nikolic, R. R.; Tomic, S. L. *Polym. Bull.* **2013**, *70*, 809.
9. Zhou, Y.; Yang, D.; Gao, X.; Chen, X.; Xu, Q.; Lu, F.; Nie, J. *Carbohydr. Polym.* **2009**, *75*, 293.

10. Shi, Y.; Lv, H.; Fu, Y.; Lu, Q.; Zhong, J.; Ma, D.; Huang, Y.; Xue, W. *Biomed. Mater.* **2013**, *8*, 055007.
11. Micic, M.; Milic, T. V.; Mitric, M.; Jokic, B.; Suljovrujic, E. *Polym. Bull.* **2013**, *70*, 3347.
12. Bako, J.; Szepesi, M.; Veres, A. J.; Cserhati, C.; Borbely, Z. M.; Hegedus, C.; Borbely, J. *Colloid Polym. Sci.* **2008**, *286*, 357. doi:10.1007/s00396-007-1793-7.
13. Glisoni, R. J.; García-Fernández, M. J.; Pino, M.; Gutkind, G.; Moglioni, A. G.; Alvarez-Lorenzo, C.; Concheiro, A.; Sosnik, A. *Carbohydr. Polym.* **2013**, *93*, 449.
14. Chang, Y.; Yandi, W.; Chen, W.-Y.; Shih, Y.-J.; Yang, C.-C.; Chang, Y.; Ling, Q.-D.; Higuchi, A. *Biomacromolecules* **2010**, *11*, 1101.
15. Noppakundilograt, S.; Sonjaipanich, K.; Thongchul, N.; Kiatkamjornwong, S. *J. Appl. Polym. Sci.* **2013**, *127*, 4927.
16. Codling, C. E.; Maillard, J. Y.; Russell, A. D. *J. Antimicrob. Chemother.* **2003**, *51*, 1153.
17. Cha, D. S.; Chinnan, M. S. *Crit. Rev. Food Sci. Nutr.* **2004**, *44*, 223.
18. Grass, G.; Rensing, C.; Solioz, M. *Appl. Environ. Microbiol.* **2011**, *77*, 1541.
19. Chan, D. I.; Prenner, E. J.; Vogel, H. J. *Biochim. Biophys. Acta Biomembr.* **2006**, *1758*, 1184.
20. Ciolino, J. B.; Hoare, T. R.; Iwata, N. G.; Behlau, I.; Dohlman, C. H.; Langer, R.; Kohane, D. S. *Invest. Ophthalmol. Vis. Sci.* **2009**, *50*, 3346.
21. Sisti, L.; Cruciani, L.; Totaro, G.; Vannini, M.; Berti, C.; Aloisio, I.; Di Gioia, D. *Prog. Org. Coat.* **2012**, *73*, 257.
22. Jones, D. S.; Lorimer, C. P.; McCoy, C. P.; Gorman, S. P. *J. Biomed. Mater. Res. B* **2008**, *85B*, 417.
23. Leung, D.; Spratt, D. A.; Pratten, J.; Gulabivala, K.; Mordan, N. J.; Young, A. M. *Biomaterials* **2005**, *26*, 7145.
24. Halpenny, G. M.; Steinhardt, R. C.; Okialda, K. A.; Mascharak, P. K. *J. Mater. Sci. Mater. Med.* **2009**, *20*, 2353.
25. Bardajee, G. R.; Hooshyar, Z.; Asli, M. J.; Shahidi, F. E.; Dianatnejad, N. *Mater. Sci. Eng. C Mater. Biol. Appl.* **2014**, *36*, 277.
26. Laverty, G.; Gorman, S. P.; Gilmore, B. F. *J. Biomed. Mater. Res. A* **2012**, *100A*, 1803.
27. Casimiro, M. H.; Leal, J. P.; Gil, M. H. *Nucl. Instrum. Methods Phys. Res. B Beam Interact. Mater. Atoms* **2005**, *236*, 482.
28. Zhou, Y.-N.; Cheng, H.; Luo, Z.-H. *AIChE J.* **2013**, *59*, 4780.
29. Fuchs, A. V.; Walter, C.; Landfester, K.; Ziener, U. *Langmuir* **2012**, *28*, 4974.
30. Zan, X.; Kozlov, M.; McCarthy, T. J.; Su, Z. *Biomacromolecules* **2010**, *11*, 1082.
31. Murthy, P. S. K.; Mohan, Y. M.; Varaprasad, K.; Sreedhar, B.; Raju, K. M. *J. Colloid Interface Sci.* **2008**, *318*, 217.
32. Paillot, P.; Becquart, F.; Jegat, C. F.; Taha, M. unpublished.
33. Martínez-Abad, A.; Lagaron, J. M.; Ocio, M. J. *J. Agric. Food Chem.* **2012**, *60*, 5350.
34. Martinez-Abad, A.; Sanchez, G.; Lagaron, J. M.; Ocio, M. J. *Colloid Polym. Sci.* **2013**, *291*, 1381.
35. Rothon, R. N. Particulate-Filled Polymer Composites, 2nd ed.; Smithers Rapra Press: Shrewsbury, UK, **2003**.
36. Logvinenko, V.; Polunina, O.; Mikhailov, Y.; Mikhailov, K.; Bokhonov, B. *J. Therm. Anal. Calorim.* **2007**, *90*, 3, 813.
37. Abu-Zied, B. M.; Asiri, A. M. *Thermochim. Acta* **2014**, *581*, 110.
38. Stara, H.; Stary, Z.; Muenstedt, H. *Macromol. Mater. Eng.* **2011**, *296*, 5, 423.
39. Obaid, A. Y.; Alyoubi, A. O.; Samarkandy, A. A.; Al-Thabaiti, S. A.; Al-Juaid, S. S.; El-Bellihi, A. A.; Deifallah, El-H. M. *J. Therm. Anal. Calorim.* **2000**, *61*, 3, 985.
40. Lin, Z.; Han, D.; Li, S. *J. Therm. Anal. Calorim.* **2011**, *107*, 2, 471.
41. Liu, Yen-Yu.; Tung, Tasn-Hua.; Liu, Kun-Ho.; Chen, San-Yuan.; Liu, Dean-Mo. *Adv. Eng. Mater.* **2009**, *11*, B219.
42. Kahveci, M. U.; Uygun, M; Odaci, D.; Timur, S.; Yagci, Y. *Macromol. Chem. Phys.* **2009**, *210*, 21, 1867.
43. Sangermano, M.; Yagci, Y.; Rizza, G. *Polymer* **2008**, *49*, 24, 5195.
44. Mark, J.; Ngai, K. L.; Graessley, W.; Mandelkern, L.; Samulksi, E.; Koenig, J.; Wigall, G., Eds.; Physical Properties of Polymers, 3rd ed.; Cambridge University Press: Cambridge, **2003**.
45. McGrath, L. M.; Parnas, R. S.; King, S. H.; Schroeder, J. L.; Fischer, D. A.; Lenhart, J. L. *Polymer* **2008**, *49*, 999.
46. Keddie, J. L.; Jones, R. A. L.; Cory, R. A. *Faraday Discuss.* **1994**, *98*, 219.
47. Fryer, D. S.; Peters, R. D.; Kim, E. J.; Tomaszewski, J. E.; de Pablo, J. J.; Nealey, P. F. *Macromolecules* **2001**, *34*, 5627.
48. Goh, C. F.; Yu, H.; Yong, S. S.; Mhaisalkar, S. G.; Boey, F. Y. C.; Teo, P. S. *Mater. Sci. Eng.* **2005**, *B117*, 153.
49. Suriati, G.; Mariatti, M.; Azizan, A. *J. Mater. Sci. Mater. Electron.* **2011**, *22*, 56.
50. Rivers, G.; Rogalsky, A.; Lee-Sullivan, P.; Zhao, B. *J. Therm. Anal. Calorim.* **2015**, *119*, 797.
51. Touhtouh, S.; Becquart, F.; Pillon, C.; Taha, M. *Polymer* **2011**, *3*, 4, 1734.
52. Hosouk, C. Chemical Incorporation of Polyhedral Oligomeric Silsesquioxane into Thermoset Matrices. Organic Chemistry. Mississippi State University, **2006**. 251 p.
53. Goekbora, B.; Pomenantz, C.; Premnath, N.; Stevenson, R. A Hydrogel Wound Dressing with Gradient Crosslinking and Silver/Copper Ions for Treatment of Severe Burns; In Bioengineering Conference (NEBEC), 39th Annual Northeast. **2013**, 237.
54. Hennink, W. E.; Talsma, H.; Borchert, J. C. H.; De Smedt, S. C.; Demeester, J. *J. Control. Release* **1996**, *39*, 1, 47.
55. Khan, S.; Ranjha, N. M. *Polym. Bull.* **2014**, *71*, 8, 2133.
56. Brahim, S.; Narinesingh, D.; Guiseppi-Elie, A. *Biomacromolecules* **2003**, *4*, 5, 1224.
57. Spizzirri, U. G.; Iemma, F.; Puoci, F.; Xue, F.; Gao, W.; Cirillo, G.; Curcio, M.; Parisi, O. I.; Picci, N. *Polym. Adv. Technol.* **2011**, *22*, 12, 1705.

58. Pittman, C. U. Jr.; Gui-Zhi, Li.; Ni, H. *Macromol. Symp.* **2002**, *196*, 1, 301.
59. Jackson, A. C.; Beyer, F. L.; Price, S. C.; Rinderspacher, B. C.; Lambeth, R. H. *Macromolecules* **2013**, 14, 5416.
60. Iatridi, Z.; Bokias, G. *Macromol. Chem. Phys.* **2008**, *209*, 10, 1029.
61. Wu, J.; Haddad, T. S.; Mather, P. T. *Macromolecules* **2009**, *42*,4, 1142.
62. Wei, Y.; Jin, D.; Yang, C.; Kels, M. C.; Qiu, K. Y. *Mater. Sci. Eng. C* **1998**, *6*, 2–3, 91.
63. Chevallier, C.; Ni, Y.; Vera, R.; Becquart, F.; Taha, M. *J. Appl. Polym. Sci.* **2013**, *129*, 1, 404.